Chemosphere 238 (2020) 124684

Contents lists available at ScienceDirect

Chemosphere

journal homepage: www.elsevier.com/locate/chemosphere

Phosphogypsum as a novel modifier for distillers grains biochar removal of phosphate from water

Bing Wang [a, b, c, *], Guoqi Lian [c, d], Xinqing Lee [c], Bin Gao [e], Ling Li [c], Taoze Liu [f], Xueyang Zhang [g], Yulin Zheng [e]

[a] College of Resource and Environmental Engineering, Guizhou University, Guiyang 550025, Guizhou, China
[b] Key Laboratory of Karst Environment and Geohazard, Ministry of Natural Resources, Guiyang, 550025 Guizhou, China
[c] State Key Laboratory of Environmental Geochemistry, Institute of Geochemistry, Chinese Academy of Sciences, Guiyang 550081, China
[d] University of Chinese Academy of Sciences, Beijing 100049, China
[e] Department of Agricultural and Biological Engineering, University of Florida, Gainesville, FL 32611, USA
[f] College of Eco-Environmental Engineering, Guizhou Minzu University, Guiyang 550025, China
[g] School of Environmental Engineering, Xuzhou University of Technology, Xuzhou 221018, China

HIGHLIGHTS

- A novel biochar composite was synthesized for phosphate adsorption.
- The maximum phosphate adsorption capacity reached 102.4 mg g^{-1}.
- The adsorption mechanism is mainly attributed to electrostatic adsorption, surface precipitation and ligand exchange.
- The composite can be used as high-quality adsorbent for phosphate removal.

ARTICLE INFO

Article history:
Received 16 July 2019
Received in revised form
5 August 2019
Accepted 25 August 2019
Available online 28 August 2019

Handling editor: J. Rinklebe

Keywords:
Distillers grains
Biochar
Phosphate adsorption
Pyrolysis
Modification

ABSTRACT

A novel biochar composite was fabricated via the pyrolysis of distillers grains treated phosphogypsum for phosphate removal from water. Batch adsorption experiments were performed on the adsorption characteristics of phosphate. Effects of pyrolysis temperature, solution pH, the dosage of adsorbent, ambient temperature on phosphate adsorption were also investigated. The results demonstrated that the optimum initial solution pH for phosphate adsorption was 6.0, and high pyrolysis temperature was favorable for phosphate adsorption. The optimal dosage of biochar was 1.25 g L^{-1}. A pseudo-second-order kinetic model can well explain the adsorption kinetics, indicative of the energetically heterogeneous solid surface of the composite. The maximum phosphate adsorption capacity of the phosphogypsum modified biochar obtained from Langmuir isotherm reached 102.4 mg g^{-1} which was almost five times that of distillers grains biochar alone (21.5 mg g^{-1}). The mechanism is mainly attributed to electrostatic adsorption, surface precipitation and ligand exchange. The ideal adsorption performance indicated that biochar supported phosphogypsum can be used as high-quality adsorbent for phosphate removal in wastewater treatment.

1. Introduction

Eutrophication of water has become a worldwide environmental problem (Le et al., 2010; Schindler David, 2012; Zhang et al., 2016). Eutrophication causes rapid propagation of algae and decreases dissolved oxygen in water bodies (Yin et al., 2018). It affects water quality as well as the health of aquatic plants and animals (Alimov and Golubkov, 2014; Li et al., 2015). Dead algae and organisms are easily oxidized in the water, which makes water be polluted and unusable (Carpenter, 2008). Phosphorus is the most important limiting factor for eutrophication (Paerl et al., 2014). It is also an indicator of surface water quality (Anderson et al., 2008; Karunanithi et al., 2017). Thus, removing phosphate from waste streams is imperative (Zheng et al., 2019). At present,

* Corresponding author. College of Resource and Environmental Engineering, Guizhou University, Guiyang 550025, Guizhou, China.
E-mail address: wangbing@vip.gyig.ac.cn (B. Wang).

https://doi.org/10.1016/j.chemosphere.2019.124684
0045-6535/

comprehensive methods have been adopted to control water eutrophication (Le et al., 2010; Garikiparthy et al., 2016). For the removal of phosphate, physicochemical methods and biological methods, such as ion exchange, coagulation-sedimentation, adsorption, electrodialysis, and artificial wetland are often used (Rittmann et al., 2011; Galvez-Cloutier et al., 2012; Zhang and Gao, 2013; Feng et al., 2017; Sophia A and Lima, 2018; Vikrant et al., 2018). Since the cost of these treatment technologies is high, more cost-effective and efficient technologies need to be developed.

Currently, carbonaceous material has become the most commonly used and effective adsorbent in the world to remove various pollutants from water. As a unique carbonaceous material, biochar is a new kind of low cost and high-efficiency adsorbent (Ahmad et al., 2012a; Shen et al., 2012). Biochar refers to a porous carbon-rich substance formed by carbonization of biomass such as agricultural and forestry wastes under low temperature pyrolysis under limited oxygen conditions (Lehmann, 2007; Lehmann and Joseph, 2015; Kan et al., 2016; Wang et al., 2016). Due to its strong stability and adsorption capacity, biochar has been widely used as an appropriate adsorbent to remove pollutants from water (Ahmad et al., 2014; Mohan et al., 2014; Wang et al., 2015a; Inyang et al., 2016; Kizito et al., 2017; Vikrant et al., 2018).

Many solid wastes can be used as raw materials for biochar. Distillers grains are fermented granules derived from distilled solids. A large amount of distillers grains are produced during the production of white wine as solid waste. They are a by-product of the brewing industry and the alcohol industry. Because of its high water content and high acidity, it is easy to corrupt and deteriorate, which not only wastes valuable resources but also results in environmental pollution (Olajire, 2012). Therefore, how to comprehensively make full use of distillers grains has become the concern of the brewing industry. It is an effective way to prepare biochar using distillers grains as feedstocks.

In recent years, many natural clay minerals, nanomaterials or other new materials have been used for the modification of biochar to enhance its adsorption capacity for pollutants (Wang et al., 2017). Some of these modification methods result in an increase in the cost of engineered biochar production due to the use of chemical reagents or nanomaterials as modifiers, thereby limiting the application of engineered biochar. Metal oxides can effectively improve the adsorption performance of biochar on phosphorus, such as magnesium, iron, aluminum, etc. Therefore, to increase biochar adsorption capacity for phosphate, a lot of research has been carried out to modify biochar by supporting metal ions such as Ca, Mg, Fe and Al. Mineral addition not only improves the retention and stability of carbon in biochar (Li et al., 2014) but also has good potential for phosphate removal from water (Liu et al., 2016; Dai et al., 2017; Saadat et al., 2018). Compared with other metal modification methods, Ca^{2+} and Mg^{2+} are the nutrients required for plants. The biochar after phosphorus adsorption contains more calcium, magnesium and phosphorus, and can be used as a soil amendment after being applied to the soil. This not only reduces soil toxicity, but also has good phosphorus removal efficiency.

Phosphogypsum (PG: $CaSO_4 \cdot 2H_2O$) is an industrial by-product produced in phosphoric acid and phosphate fertilizer production (Rashad, 2017). It is estimated that world production of this waste exceeds 160–280 million tons per year (Rutherford et al., 1994). The massive discharge of phosphogypsum not only occupies a large area of land but also poses a great threat to environmental safety and the health of residents. Therefore, how to utilize phosphogypsum effectively has become an important problem world widely (Rutherford et al., 1994; Tayibi et al., 2009). As a calcium-rich substance, phosphogypsum may change the functional groups, surface charges of biochar after being attached to the surface of biochar, thus affecting its adsorption capacity for pollutants.

Based on the above idea, we assume that phosphogypsum modification of distillers grains biochar can improve its adsorption capacity to aqueous phosphate. The aims of this study are to (1) fabricate a novel adsorbent for phosphate adsorption in water; (2) examine the effects of pH and adsorbent dosage on phosphate adsorption, and (3) determine the adsorption kinetics and isotherms of phosphate adsorption.

2. Materials and methods

2.1. Chemicals and reagents

Reagents including potassium dihydrogen phosphate (KH_2PO_4) (Acros), sulfuric acid (H_2SO_4), sodium hydroxide (NaOH), ascorbic acid ($C_6H_8O_6$), potassium antimony tartrate ($KSbC_4H_4O_7 \cdot 1/2H_2O$), and ammonium molybdate ($(NH_4)_6Mo_7O_{24} \cdot 4H_2O$] were obtained from Tianjin Kermel Chemical Reagent Co., Ltd.

2.2. Preparation of biochar

Distillers grains were sampled from a local distillery, Guizhou province, China. Phosphogypsum was collected from a phosphate fertilizer plant, Guizhou province, China. The distillers grains and phosphogypsum were dried in the oven to constant weight at 105 °C. The dried phosphogypsum and distillers grains were mixed in a weight ratio of 1:2, and then uniformly mixed with an equal volume of water, and dried in an oven at 105 °C. Biochar was prepared from a mixture of distillers grains and phosphogypsum in a Tubular carbonization furnace. The treated raw materials were pyrolyzed at 300 °C, 400 °C, 500 °C, and 600 °C, respectively under a nitrogen atmosphere. The residence time and heating rate are the same as our previous study (Wang et al., 2015a). Biochar prepared at different pyrolysis temperatures were labeled as: Distillers grains biochar (300 °C), Distillers grains biochar (400 °C), Distillers grains biochar (500 °C), Distillers grains biochar (600 °C), PG-biochar (300 °C),PG-biochar (400 °C), PG-biochar (500 °C), and PG-biochar (600 °C).

2.3. Determination of physicochemical properties of biochars

The pH value of biochar samples was determined with a biochar-to-water ratio of 1:20 (w/v). The electrical conductivity (EC) of biochar was determined by weighing 1.0 g of biochar sample and adding 20 mL of ultrapure water. After shaking for 1 h, and the supernatant was filtered with a 0.45 μm nylon filter. The EC of the filtrate was determined using a portable EC meter (HANNA HI9033). Proximate analysis was performed using ASTM D1762-84 Chemical Analysis of Wood Charcoal (ASTM, 2007). The surface zeta potential values of the biochars were measured by a Malvern Zeta meter (Nano ZSE + MPT2, Malvern Panalytical Instruments Ltd., UK).

Surface morphology of biochars was determined using a scanning electron microscope (SEM) (JSM-6460 LV Scanning Microscope (JEOL, Tokyo, Japan). The surface functional groups of the biochars were determined using a Nicolet iS50 Fourier transform infrared (FTIR) (Thermo Fisher Scientific, USA). In order to get the detectable FTIR spectrum, the biochar was ground up, blended with KBr to 0.1 wt%, and afterward pressed into the pellets. Infrared spectra were obtained at room temperature (22 ± 0.5 °C) in the spectral range from 400 cm^{-1}–4000 cm^{-1}. Elemental C H N analyses were completed using a CHN elemental analyzer (Elementar Vario MACRO).

2.4. Adsorption experiments

The adsorption experiment was carried out in a 50 mL PE centrifugal tube at room temperature (22 ± 0.5 °C). The concentration of phosphate was determined by the ascorbic acid method (American Public Health Association, 2017), and the absorbance of 700 nm was determined by UV−vis spectrophotometer (V-1600, Shanghai Mapada Instruments Co., Ltd, China).

In order to choose the optimal adsorbent dosage, the adsorption experiment was performed with an adsorbent dosage of 0.0250 g/40 mL, 0.0500 g/40 mL, 0.1000 g/40 mL, and 0.2000 g/40 mL, respectively. The supernatant was taken and phosphate concentration was measured immediately after filtration with 0.45 μm nylon filter.

The effect of pH on phosphate adsorption was analyzed with initial pH of 100 mg L^{-1} phosphate solutions adjusted to 3.0, 4.0, 5.0, 6.0, 7.0, 8.0, 9.0, 10.0, 11.0 and 12.0 using 0.1 M H_2SO_4 and 0.1 M NaOH solution. Sorption kinetics of phosphate was analyzed by phosphate standard solution at an interval time between 0.083 and 24 h, respectively. Sorption isotherms were examined at different concentrations between 5 and 500 mg L^{-1}. Adsorption thermodynamics were conducted in the ambient temperature of 16 °C, 26 °C and 36 °C. The measurement methods and procedures are the same as described above.

3. Results and discussion

3.1. Characterization of the samples

The physicochemical properties of distillers grains biochar and PG-biochar are shown in Table S1, both biochars were alkaline. From the point of chargeability, the distillers grains were negatively charged, and the modified biochar was positively charged. It is indicated that the distillers grains biochar modified by phosphogypsum has electrostatic adsorption to the negatively charged phosphate. After the modification, the electrical conductivity (EC) was greatly improved. This indicates that conductive ions are generated after the phosphogypsum is doped to the surface of the distillers grains biochar, which causes an increase in EC. Compared with the distillers grains biochar, the PG-biochar had a higher H/C value, indicating that its structure contains abundant functional groups (Ahmad et al., 2012a). Surface morphologies of the distillers grains biochar and PG-biochars pyrolyzed at different temperatures as well as phosphogypsum are shown in Fig. S1. Many phosphogypsum particles were found on the surface of distillers grains biochar after pyrolysis.

To further demonstrate that the phosphate does adsorb on the surface of PG-biochar, the SEM-EDS analysis of biochar samples before and after adsorption was performed. It can be seen from the SEM-EDS images in Fig. 1 that the biggest difference between the 600 °C distillers grains biochar and the modified biochar is that the carbon content of the distillers grains biochar is much higher than that of the modified biochar. After the adsorption of phosphorus, phosphorus content in the distillers grains biochar did not change too much, while the content of phosphorus in the modified biochar increased greatly after the adsorption, indicating that the modified biochar had obvious adsorption effect on phosphate. The SEM-EDS spectra of the PG-biochar also showed the presence of more Ca and S compared to that of distillers grains biochars. The results indicated that the precipitation of calcium-phosphate might be an important mechanism for phosphate removal. Moreover, the zeta potential of PG-biochar is higher than distillers grains biochar. Protonation may occur on the PG-biochar surface which creates a partial positive charge helping phosphate sorption via electrostatic attraction.

Fig. 2 shows the infrared spectrum of different biochars before adsorption. In the Fourier transform infrared spectroscopy of all biochars, there is an absorption peak between the wavenumbers of 3600-3300 cm^{-1}, which is mainly caused by the intermolecular hydrogen bond-associated alcohol and the phenol-OH stretching vibration. The absorption peaks at a wavenumber of 1600−1670 cm^{-1} are mainly C═O and conjugated aromatic ring stretching C═C (Angın, 2013). In the infrared spectrum of PM-biochar, we can clearly see that there are distinct absorption peaks between the wavenumbers of 1635, 1065 and 698 cm^{-1}. Among them, the characteristic peak with an absorption peak of 1635 cm^{-1} may be the carbonyl group of the carboxyl group in biochar. A vibrating zone with a wavenumber of approximately 1065 cm^{-1} indicates that the biochar contains C═O, C═C, and C−O bonds. A vibration band with a wavenumber of approximately 600 cm^{-1} indicates the presence of an aromatic C−H bond. The characteristic peak of 698 cm^{-1} is generated by Ca−O stretching vibration, which indicates that Ca is successfully embedded in the biochar as CaO or $Ca(OH)_2$. The SEM-EDS, Zeta potential and FTIR results indicated that the phosphate sorption mechanisms may involve surface precipitation and electrostatic attraction.

3.2. Effect of pyrolysis temperature

Pyrolysis conditions directly affect the physicochemical properties of biochar (Wang et al., 2016). The adsorption of phosphate by PG-biochar increased as the pyrolysis temperature increased, while there is no considerable difference between the adsorption capacity of distillers grains biochar (Fig. 3). This may be due to the fact that the pyrolysis temperature largely affects the surface morphology of the biochar. As the pyrolysis temperature increased, a large amount of energy was released from the interior of the raw material, and the internal pores were opened. The pore distribution of the biochar became disordered, increasing the surface roughness and area, which is beneficial for phosphate adsorption (Ahmad et al., 2012b).

3.3. Effects of dosage

The adsorption and removal rate of phosphate by biochar are shown in Fig. S2. Under the same initial concentration of phosphate, the adsorption amount increased initially and then decreased. The removal rate of phosphate by biochar sharply increased when the dosage shifted from 0.0200 g/40 mL to 0.0500 g/40 mL, and then gradually raised and kept it at around 95%. When the dosage of adsorbent continued to increase, the phosphate removal rate did not change much. This is due to an increase in the dosage of adsorbent, which increases the effective functional groups and the adsorbed active sites. When the dosage was 0.0500 g/40 mL, the maximum adsorption amount was reached. From the perspective of economic costs, the optimum dosage is 0.0500 g/40 mL.

3.4. pH effect on phosphate adsorption

Previous studies have shown that solution pH is a key factor affecting phosphate adsorption (Cui et al., 2011). In this study, the effect of pH on the adsorption of phosphate by two different adsorbents in the range of 3.0−12.0 was investigated. For both biochars, the maximum adsorption amount was at pH = 6 (Fig. S3).

When the initial solution pH is less than 3, phosphate mainly exists in the form of H_3PO_4 (pKa = 2.12, pKa is the negative logarithm of the acid dissociation constant), and the binding force of H_3PO_4 to biochar is weak (Zhang et al., 2011). Although the phosphate removal rate was high, the adsorption amount was only

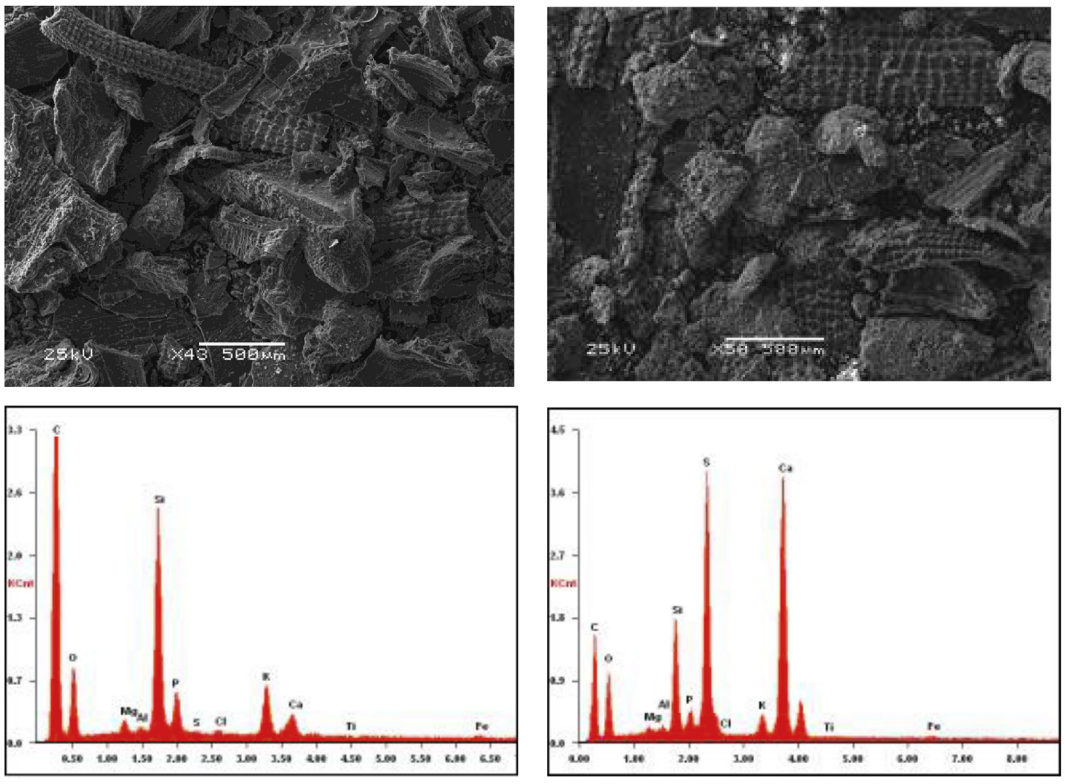

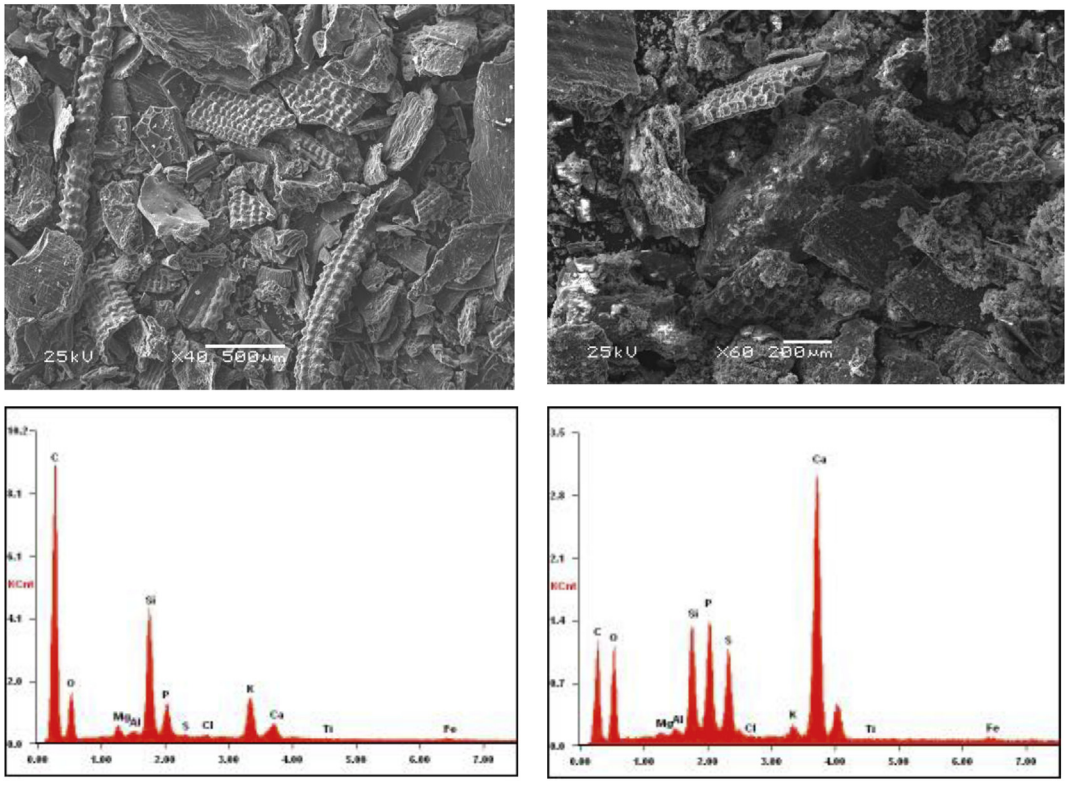

Fig. 1. SEM images of distillers grains biochar and PG-biochar pyrolyzed under 600 °C before and after absorption of phosphate.

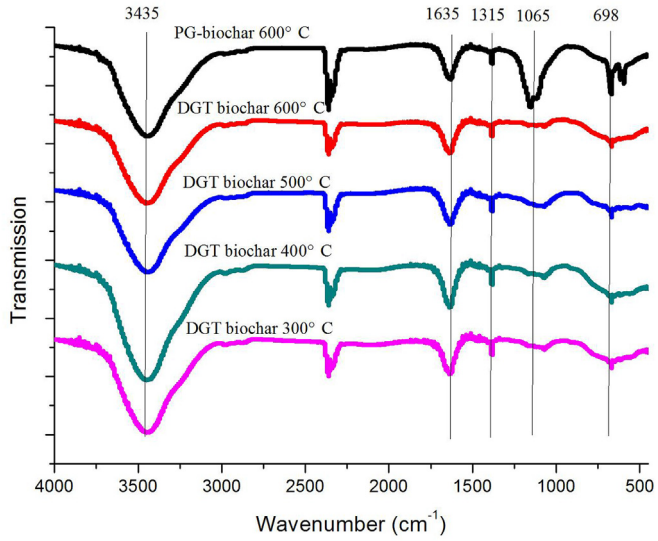

Fig. 2. FTIR spectra of different biochars (PG-biochar means phosphogypsum supported distillers grains biochar, DGT biochar means distillers grains biochar).

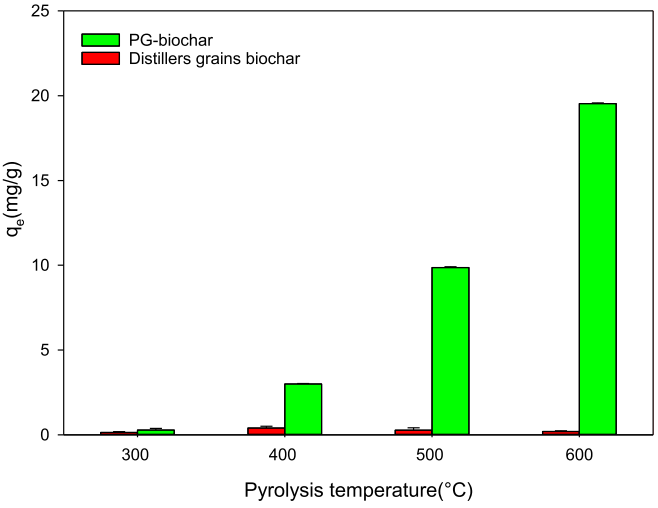

Fig. 3. Adsorption of phosphate by biochar pyrolysis at different temperatures. Error bars represent standard error of triplicate samples (n = 3). Initial phosphate concentration 100 mg L^{-1}. Contact time 24 h.

75 mg g^{-1}. When the pH was between 3 and 7, the phosphate removal rate reached a maximum (96.7%) at pH = 6. At the same time, the amount of adsorbed phosphate reached a maximum of 79 mg g^{-1} probably because phosphate was mainly present in the form of $H_2PO_4^-$ (pKa = 7.21). $H_2PO_4^-$ may have strong interactions with the hydroxyl groups on the surface of phosphogypsum/biochar through ligand exchange (Chen et al., 2012).

When the pH of the solution was between 8 and 12, the phosphate removal rate was between 83% and 86%. Phosphate mainly existed in the form of HPO_4^{2-} (pKa = 12.67). The high concentration of OH^- in the solution might inhibit the coordination of hydroxyl groups on the biochar with HPO_4^{2-}. The exchange between the bodies may compete with the HPO_4^{2-} in the solution for the adsorption site on the surface of the biochar. Since the zero point charge pH_{pzc} of the modified distillers grains biochar is 7.74, the modified biochar surface is positively charged when $pH < pH_{pzc}$, and it is easier to adsorb anions through electrostatic adsorption. As the pH increases, the OH^- concentration increases rapidly, which is competitive with the phosphate and not conducive to the adsorption. Therefore, based on the result of the removal rate and adsorption capacity of biochar on phosphate, all subsequent sorption experiments were conducted at pH = 6.0.

3.5. Adsorption kinetics

The adsorption kinetics data were simulated by different mathematical models. In addition to the commonly used pseudo-first-order, pseudo-second-order models, Elovich model, and Ritchie model were tested with the following equation (Ho, 2006; Zhang et al., 2013).

$$q_t = q_e\left(1 - e^{-kt}\right) \text{ Pseudo} - \text{first} - \text{order model} \quad (1)$$

$$q_t = \frac{kq_e^2 t}{1 + kq_e t} \text{Pseudo} - \text{second} - \text{order model} \quad (2)$$

$$q_t = \frac{1}{\beta}\ln(\beta\alpha t + 1) \text{ Elovich model} \quad (3)$$

$$q_t = q_e - \left(q_e^{1-n} - \frac{k}{1-n}t\right)^{\frac{1}{1-n}} \text{ Ritchie model} \quad (4)$$

As shown in Fig. 4, the adsorption rate of phosphate was very fast at the beginning. The adsorption of phosphate increased rapidly in the first 4 h, reaching 70% of the maximum adsorption amount, then the curve slowly slowed down and finally reached the adsorption equilibrium at 24 h. Under the same initial phosphate concentration, the concentration of phosphate decreased with the process of adsorption, and the diffusion rate of phosphate decreased, which leads to the increase of the thickness of the boundary layer and abruptly changes. The decrease of phosphate concentration can be attributed to the calcium-induced calcium phosphate precipitation. Overall, the pseudo-second-order model provided the best fit of the experimental data for both adsorbents (Table S2), indicating that phosphate adsorption kinetics by distillers grains biochar or PG-biochar was mostly through chemical sorption process.

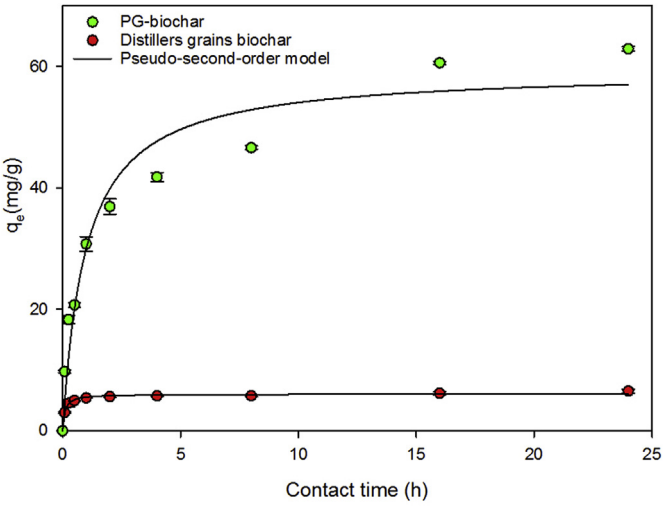

Fig. 4. The relationship between the amount of phosphate adsorption and the contact time. Error bars represent standard error of triplicate samples (n = 3). Symbols may cover error bars. Initial phosphate concentration 100 mg L^{-1}. Contact time 24 h.

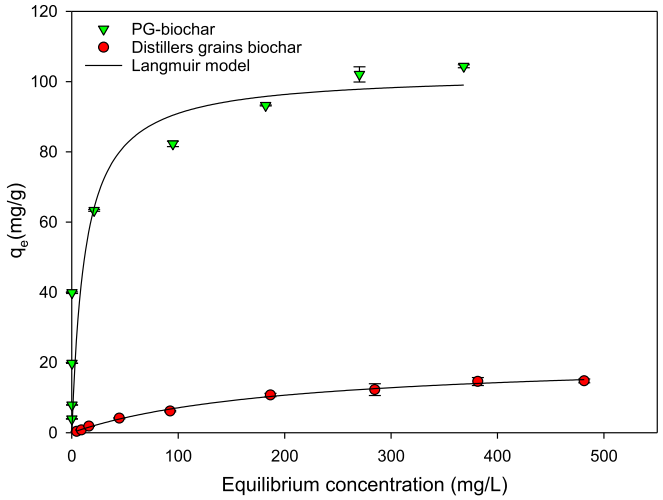

Fig. 5. Adsorption isotherms of phosphate onto adsorbents. Error bars represent standard error of triplicate samples (n = 3). Symbols may cover error bars. Initial phosphate concentration 5–500 mg L^{-1}. Contact time 24 h.

3.6. Adsorption isotherms

Two isotherm models were used to simulate the adsorption of phosphate from biochar.

$$S = \frac{S_{max} KC}{1 + KC} \text{ Langmuir model} \quad (5)$$

$$S = K_f C^n \text{ Freundlich model} \quad (6)$$

The phosphate adsorption capacity of biochar increased with the increase of initial phosphate equilibrium concentration (Fig. 5). This is because the amount of phosphate contacting between the solid and liquid phases is increased so that the reactivity of the adsorption site on the surface of the adsorbent is enhanced. As the initial phosphate concentration increased, the phosphate exposed to per unit biochar mass increased, resulting in more active sites to be occupied. Table S3 shows the best-fit parameters of these isotherm models. According to the fitting curves, both models fit well on the phosphorus adsorption process. While the adsorption process of PG-biochar is more consistent with the Freundlich isotherm adsorption model, which belongs to the monolayer surface chemisorption. This is consistent with the results of previous studies of phosphate removal by other adsorbents (Zhang et al., 2012, 2013). The maximum adsorption capacity of PG-biochar reached 102.4 mg g^{-1}, which is almost five times that of distillers grains biochar (21.5 mg g^{-1}). The Langmuir constants k_L is between 0.005 and 0.08 mg L^{-1}, indicating that the adsorption of phosphate by biochar was chemisorption, while the Freundlich constant was more than 1 indicating that the phosphorus adsorption is primarily a single layer chemical adsorption of the surface of PG-biochar. The higher adsorption capacity of PG-biochar than distillers grains biochar is partly due to a large amount of divalent cation (Ca^{2+}) bridging of phosphate on the surface of biochar contributing greatly to the precipitation of phosphate ions. Another possible phosphate adsorption mechanism on the biochar surface could be attributed to ligand exchange reaction between the phosphate-hydroxyl surface reaction.

The adsorption capacity of PG-biochar on phosphate is almost comparable to that of other modified biochars (Table 1). Although the phosphate adsorption capacity obtained in this study was not as high as some previous works, the most remarkable point is that the PG-biochar is low cost and modification method is simple. Because both distillers grains and phosphogypsum belong to solid wastes, PG-biochar could be widely used as a very cost-effective and novel adsorbent due to the perspective of solid waste management.

3.7. Adsorption thermodynamics

By studying some thermodynamic parameters, we can deduce the possibility and extent of adsorption reactions. The thermodynamics of phosphate adsorption on the PG-biochar at 289.15 K, 299.15 K, and 309.15 K were analyzed. As shown in Fig. 6, the adsorbed amount of phosphorus increased with the increase of ambient temperature, indicating that the phosphate adsorption process is chemical. In order to understand the adsorption process more comprehensively, some thermodynamic data calculation is needed. The Freundlich model was used to calculate the differential enthalpy of adsorption, adsorption free energy, and adsorption entropy. The thermodynamic equations can be written as follows (Huang et al., 2014).

Table 1
Previously reported adsorption capacities of phosphate onto various biochar.

Biochar	Temperature (°C)	Q_0 (mg g^{-1})	pH	Ref
Oak sawdust biochar by Lanthanum (La)-involved	500	142.7		Wang et al. (2015b)
Anaerobically digested sugar beet tailings biochar	600	100	5.2	Yao et al. (2011a)
Mixed hardwood feedstock biochar	300	1.13		Sarkhot et al. (2013)
Mg-enriched tomato tissues biochar	600	>100		Yao et al. (2013b)
Anaerobically digested sugar beet tailings biochar	600	133	5.2	Yao et al. (2011b)
Biochar/AlOOH nanocomposite	600	120		Zhang and Gao (2013)
MgO-biochar nanocomposites	600	835		Zhang et al. (2012)
Magnesium ferrite ($MgFe_2O_4$)/biochar magnetic composites	800	163.02	3.0	Jung et al. (2017)
Soybean stover derived biochar	700	90.9	5.5	Karunanithi et al. (2017)
MgO particle-impregnated biochar	500	398	4.0	Li et al. (2017)
Montmorillonite/bamboo biochar	400	105.28		Chen et al. (2017)
Tomato leaves biochar	600	116.6	5.2	Yao et al. (2013a)
Poultry manure biochar	650	163.6		Novais et al. (2018)
Magnesium-pretreated biochar	600	66.7	5.2	Haddad et al. (2018)
MgO decorated magnetic biochar	550	121.25	4.0	Li et al. (2016b)
Rice straw-derived biochar	600	40	3.0	Cui et al. (2011)
Magnesium-alginate/chitosan modified biochar	500	46.56	3.0	Cui et al. (2016)
Wheat straw biochar	450	16.58	7.0	Li et al. (2016a)
Distillers grains biochar	600	21.5	6.0	This study
PG-biochar	600	102.4	6.0	This study

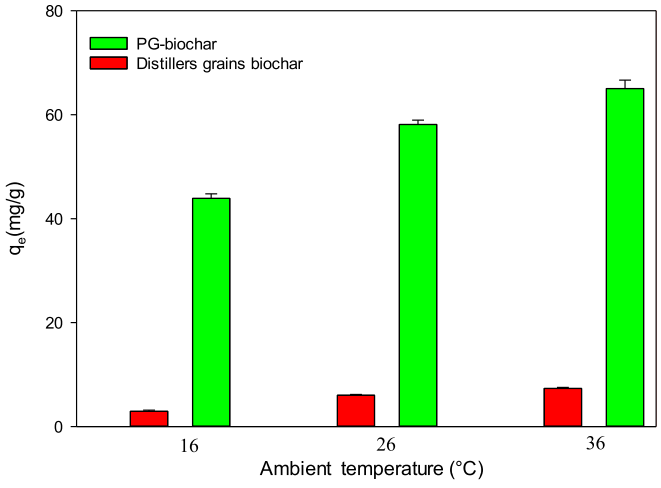

Fig. 6. The relationship between adsorption capacity and ambient temperature. Error bars represent standard error of triplicate samples (n = 3). Initial phosphate concentration 100 mg L^{-1}. Contact time 24 h.

$$\Delta G^0 = -RT\ln K_d \quad (7)$$

$$\Delta G^0 = \Delta H^0 - T\Delta S^0 \quad (8)$$

Equation (9) is obtained from the rearrangement of Eqs. (7) and (8):

$$\ln Kd = \frac{\Delta S^0}{R} - \frac{\Delta H^0}{RT} \quad (9)$$

In the above equation, ΔG^0, ΔH^0, and ΔS^0 represent the Gibbs free energy change (kJ·mol^{-1}), enthalpy change (kJ·mol^{-1}) and entropy change (J·mol^{-1}) of biochar on the isothermal adsorption process of phosphate, respectively; R is the ideal gas state equation constant 8.314 J mol^{-1} K^{-1}; T is the thermodynamic temperature, K; K_d is the adsorption equilibrium constant (K) from the value of the best fit nonlinear isotherm equilibrium model (Lima et al., 2015), which is calculated using the method recommended by Eder C. Lima et al. (2019).

At the three temperatures, the ΔG^0 in the process of biochar adsorption of phosphate was negative and gradually decreased with the increase of temperature. The ΔH^0 and ΔS^0 in the process of biochar adsorption of phosphate were both positive (Table S4). The negative values of ΔG^0 from −7.813 to −9.381 kJ mol^{-1} indicate that the adsorption of phosphate onto PG-biochar is feasible and spontaneous, and a larger negative value indicates that the reaction proceeds more thoroughly and more phosphate adsorbed with the increasing temperature (Mezenner and Bensmaili, 2009). The positive value of ΔS^0 reflects good affinity of phosphate ions towards the PG-biochar and the increasing spontaneity (randomness) of liquid-solid phase interaction at the biochar surface during the adsorption process. In the system composed of biochar and phosphate, biochar can adsorb phosphate more firmly. The ΔH^0 is positive, indicating that the phosphate adsorption process is primarily endothermic and chemical. The above results indicate that: (1) the adsorption process of phosphate on biochar is a spontaneous endothermic process, and the increase of temperature is beneficial to increase the adsorption capacity of biochar to phosphate; (2) the adsorption of biochar to phosphate is relatively firm; (3) The adsorption of phosphate on biochar is mainly chemical adsorption, supplemented by physical adsorption.

4. Conclusions

Distillers grains biochar supported phosphogypsum composites could be a novel and effective adsorbent for removal of phosphate from water. The optimum pH for phosphate adsorption was 6.0 for biochar supported phosphogypsum composites. Langmuir model can better fit the isothermal adsorption data and the maximum phosphate adsorption capacity of the phosphogypsum modified biochar reached 102.4 mg g^{-1}, which is almost five times that of the distillers grains biochar. The main adsorption mechanism is mainly attributed to electrostatic adsorption, surface precipitation and ligand exchange. The preparation method of the biochar supported phosphogypsum composite is simple and easy, and the cost is low which provides an alternative way for expanding the resource utilization of industrial wastes such as distillers grains and phosphogypsum in treating eutrophic water.

Acknowledgments

This project was supported by the National Key Research and Development Program of China (2016YFC0502602), the High-Level Overseas Talent Innovation and Entrepreneurship Project of Guizhou Province (201808) and the Opening Fund of State Key Laboratory of Environmental Geochemistry (SKLEG2019704).

Appendix A. Supplementary data

Supplementary data to this article can be found online at https://doi.org/10.1016/j.chemosphere.2019.124684.

References

Ahmad, M., Lee, S.S., Dou, X., Mohan, D., Sung, J.-K., Yang, J.E., Ok, Y.S., 2012a. Effects of pyrolysis temperature on soybean stover- and peanut shell-derived biochar properties and TCE adsorption in water. Bioresour. Technol. 118, 536–544.
Ahmad, M., Lee, S.S., Dou, X., Mohan, D., Sung, J.-K., Yang, J.E., Ok, Y.S., 2012b. Effects of pyrolysis temperature on soybean stover-and peanut shell-derived biochar properties and TCE adsorption in water. Bioresour. Technol. 118, 536–544.
Ahmad, M., Rajapaksha, A.U., Lim, J.E., Zhang, M., Bolan, N., Mohan, D., Vithanage, M., Lee, S.S., Ok, Y.S., 2014. Biochar as a sorbent for contaminant management in soil and water: a review. Chemosphere 99, 19–33.
Alimov, A.F., Golubkov, M.S., 2014. Lake eutrophication and community structure. Inland. Water. Biol 7, 185–191.
American Public Health Association, A.W.W.A., Water Environmental Federation, 2017. Standard Methods for the Examination of Water and Wastewater, 23rd Edition. American Public Health Association (APHA). American Public Health Association, Washington, DC, USA.
Anderson, D.M., Burkholder, J.M., Cochlan, W.P., Glibert, P.M., Gobler, C.J., Heil, C.A., Kudela, R.M., Parsons, M.L., Rensel, J.J., Townsend, D.W., 2008. Harmful algal blooms and eutrophication: examining linkages from selected coastal regions of the United States. Harmful Algae 8, 39–53.
Angın, D., 2013. Effect of pyrolysis temperature and heating rate on biochar obtained from pyrolysis of safflower seed press cake. Bioresour. Technol. 128, 593–597.
ASTM, 2007. D1762-84 Standard Test Method for Chemical Analysis of Wood Charcoal. ASTM International, Conshohocken,PA.
Carpenter, S.R., 2008. Phosphorus control is critical to mitigating eutrophication. P.Natl. Acad. Sci. USA 105, 11039–11040.
Chen, L., Chen, X.L., Zhou, C.H., Yang, H.M., Ji, S.F., Tong, D.S., Zhong, Z.K., Yu, W.H., Chu, M.Q., 2017. Environmental-friendly montmorillonite-biochar composites: facile production and tunable adsorption-release of ammonium and phosphate. J. Clean. Prod. 156, 648–659.
Chen, N., Feng, C., Zhang, Z., Liu, R., Gao, Y., Li, M., Sugiura, N., 2012. Preparation and characterization of lanthanum(III) loaded granular ceramic for phosphorus adsorption from aqueous solution. J.Taiwan.Inst.Chem.E. 43, 783–789.
Cui, H.-J., Wang, M.K., Fu, M.-L., Ci, E., 2011. Enhancing phosphorus availability in phosphorus-fertilized zones by reducing phosphate adsorbed on ferrihydrite using rice straw-derived biochar. J.Soil.Sediment. 11, 1135.
Cui, X., Dai, X., Khan, K.Y., Li, T., Yang, X., He, Z., 2016. Removal of phosphate from aqueous solution using magnesium-alginate/chitosan modified biochar microspheres derived from Thalia dealbata. Bioresour. Technol. 218, 1123–1132.
Dai, L., Tan, F., Li, H., Zhu, N., He, M., Zhu, Q., Hu, G., Wang, L., Zhao, J., 2017. Calcium-rich biochar from the pyrolysis of crab shell for phosphorus removal. J. Environ. Manag. 198, 70–74.
Feng, Y., Lu, H., Liu, Y., Xue, L., Dionysiou, D.D., Yang, L., Xing, B., 2017. Nano-cerium

oxide functionalized biochar for phosphate retention: preparation, optimization and rice paddy application. Chemosphere 185, 816–825.
Galvez-Cloutier, R., Saminathan, S.K., Boillot, C., Triffaut-Bouchet, G., Bourget, A., Soumis-Dugas, G., 2012. An evaluation of several in-lake restoration techniques to improve the water quality problem (eutrophication) of Saint-Augustin Lake, Quebec, Canada. Environ. Manag. 49, 1037–1053.
Garikiparthy, P.S.N., Lee, S.C., Liu, H., Kolluri, S.S., Esfahani, I.J., Yoo, C.K., 2016. Evaluation of multiloop chemical dosage control strategies for total phosphorus removal of enhanced biological nutrient removal process. Korean J. Ceram. 33, 14–24.
Haddad, K., Jellali, S., Jeguirim, M., Trabelsi, A.B.H., Limousy, L., 2018. Investigations on phosphorus recovery from aqueous solutions by biochars derived from magnesium-pretreated cypress sawdust. J. Environ. Manag. 216, 305–314.
Ho, Y.-S., 2006. Review of second-order models for adsorption systems. J. Hazard Mater. 136, 681–689.
Huang, W.-Y., Li, D., Liu, Z.-Q., Tao, Q., Zhu, Y., Yang, J., Zhang, Y.-M., 2014. Kinetics, isotherm, thermodynamic, and adsorption mechanism studies of La $(OH)_3$-modified exfoliated vermiculites as highly efficient phosphate adsorbents. Chem. Eng. J. 236, 191–201.
Inyang, M.I., Gao, B., Yao, Y., Xue, Y., Zimmerman, A., Mosa, A., Pullammanappallil, P., Ok, Y.S., Cao, X., 2016. A review of biochar as a low-cost adsorbent for aqueous heavy metal removal. Crit. Rev. Environ. Sci. Technol. 46, 406–433.
Jung, K.-W., Lee, S., Lee, Y.J., 2017. Synthesis of novel magnesium ferrite $(MgFe_2O_4)$/biochar magnetic composites and its adsorption behavior for phosphate in aqueous solutions. Bioresour. Technol. 245, 751–759.
Kan, T., Strezov, V., Evans, T.J., 2016. Lignocellulosic biomass pyrolysis: a review of product properties and effects of pyrolysis parameters. Renew. Sustain. Energy Rev. 57, 1126–1140.
Karunanithi, R., Ok, Y.S., Dharmarajan, R., Ahmad, M., Seshadri, B., Bolan, N., Naidu, R., 2017. Sorption, kinetics and thermodynamics of phosphate sorption onto soybean stover derived biochar. Environmental Technology & Innovation 8, 113–125.
Kizito, S., Luo, H., Wu, S., Ajmal, Z., Lv, T., Dong, R., 2017. Phosphate recovery from liquid fraction of anaerobic digestate using four slow pyrolyzed biochars: dynamics of adsorption, desorption and regeneration. J. Environ. Manag. 201, 260–267.
Le, C., Zha, Y., Li, Y., Sun, D., Lu, H., Yin, B., 2010. Eutrophication of lake waters in China: cost, causes, and control. Environ. Manag. 45, 662–668.
Lehmann, J., 2007. A handful of carbon. Nature 447, 143–144.
Lehmann, J., Joseph, S., 2015. Biochar for Environmental Management: Science, Technology and Implementation. Routledge.
Li, F., Cao, X., Zhao, L., Wang, J., Ding, Z., 2014. Effects of mineral additives on biochar formation: carbon retention, stability, and properties. Environ. Sci. Technol. 48, 11211–11217.
Li, J.-h., Lv, G.-h., Bai, W.-b., Liu, Q., Zhang, Y.-c., Song, J.-q., 2016a. Modification and use of biochar from wheat straw (Triticum aestivum L.) for nitrate and phosphate removal from water. Desalin.Water.Treat 57, 4681–4693.
Li, R., Wang, J.J., Zhou, B., Awasthi, M.K., Ali, A., Zhang, Z., Lahori, A.H., Mahar, A., 2016b. Recovery of phosphate from aqueous solution by magnesium oxide decorated magnetic biochar and its potential as phosphate-based fertilizer substitute. Bioresour. Technol. 215, 209–214.
Li, R., Wang, J.J., Zhou, B., Zhang, Z., Liu, S., Lei, S., Xiao, R., 2017. Simultaneous capture removal of phosphate, ammonium and organic substances by MgO impregnated biochar and its potential use in swine wastewater treatment. J. Clean. Prod. 147, 96–107.
Li, X., Xu, Y., Zhao, G., Shi, C., Wang, Z.-l., Wang, Y., 2015. Assessing threshold values for eutrophication management using Bayesian method in Yuqiao Reservoir, North China. Environ. Monit. Assess. 187, 195.
Lima, É.C., Adebayo, M.A., Machado, F.M., 2015. Kinetic and Equilibrium Models of Adsorption. Carbon Nanomaterials as Adsorbents for Environmental and Biological Applications. Springer, pp. 33–69.
Lima, E.C., Hosseini-Bandegharaei, A., Moreno-Piraján, J.C., Anastopoulos, I., 2019. A critical review of the estimation of the thermodynamic parameters on adsorption equilibria. Wrong use of equilibrium constant in the Van't Hoof equation for calculation of thermodynamic parameters of adsorption. J. Mol. Liq. 273, 425–434.
Liu, S.-b., Tan, X.-f., Liu, Y.-g., Gu, Y.-l., Zeng, G.-m., Hu, X.-j., Wang, H., Zhou, L., Jiang, L.-h., Zhao, B.-b., 2016. Production of biochars from Ca impregnated ramie biomass (Boehmeria nivea (L.) Gaud.) and their phosphate removal potential. RSC Adv. 6, 5871–5880.
Mezenner, N.Y., Bensmaili, A., 2009. Kinetics and thermodynamic study of phosphate adsorption on iron hydroxide-eggshell waste. Chem. Eng. J. 147, 87–96.
Mohan, D., Sarswat, A., Ok, Y.S., Pittman Jr., C.U., 2014. Organic and inorganic contaminants removal from water with biochar, a renewable, low cost and sustainable adsorbent – a critical review. Bioresour. Technol. 160, 191–202.
Novais, S.V., Zenero, M.D.O., Tronto, J., Conz, R.F., Cerri, C.E.P., 2018. Poultry manure and sugarcane straw biochars modified with $MgCl_2$ for phosphorus adsorption. J. Environ. Manag. 214, 36–44.
Olajire, A.A., 2012. The brewing industry and environmental challenges. J. Clean. Prod. https://doi.org/10.1016/j.jclepro.2012.1003.1003.
Paerl, H.W., Hall, N.S., Peierls, B.L., Rossignol, K.L., 2014. Evolving paradigms and challenges in estuarine and coastal eutrophication dynamics in a culturally and climatically stressed world. Estuar. Coasts 37, 243–258.
Rashad, A.M., 2017. Phosphogypsum as a construction material. J. Clean. Prod. 166, 732–743.
Rittmann, B.E., Mayer, B., Westerhoff, P., Edwards, M., 2011. Capturing the lost phosphorus. Chemosphere 84, 846–853.
Rutherford, P.M., Dudas, M.J., Samek, R.A., 1994. Environmental impacts of phosphogypsum. Sci. Total Environ. 149, 1–38.
Saadat, S., Raei, E., Talebbeydokhti, N., 2018. Enhanced removal of phosphate from aqueous solutions using a modified sludge derived biochar: comparative study of various modifying cations and RSM based optimization of pyrolysis parameters. J. Environ. Manag. 225, 75–83.
Sarkhot, D., Ghezzehei, T., Berhe, A., 2013. Effectiveness of biochar for sorption of ammonium and phosphate from dairy effluent. J. Environ. Qual. 42, 1545–1554.
Schindler David, W., 2012. The dilemma of controlling cultural eutrophication of lakes. P. Roy. Soc. Lond. B. Bio 279, 4322–4333.
Shen, Y.-S., Wang, S.-L., Tzou, Y.-M., Yan, Y.-Y., Kuan, W.-H., 2012. Removal of hexavalent Cr by coconut coir and derived chars–The effect of surface functionality. Bioresour. Technol. 104, 165–172.
Sophia, A.,C., Lima, E.C., 2018. Removal of emerging contaminants from the environment by adsorption. Ecotoxicol. Environ. Saf. 150, 1–17.
Tayibi, H., Choura, M., López, F.A., Alguacil, F.J., López-Delgado, A., 2009. Environmental impact and management of phosphogypsum. J. Environ. Manag. 90, 2377–2386.
Vikrant, K., Kim, K.-H., Ok, Y.S., Tsang, D.C.W., Tsang, Y.F., Giri, B.S., Singh, R.S., 2018. Engineered/designer biochar for the removal of phosphate in water and wastewater. Sci. Total Environ. 616–617, 1242–1260.
Wang, B., Gao, B., Fang, J., 2017. Recent advances in engineered biochar productions and applications. Crit. Rev. Environ. Sci. Technol. 47, 2158–2207.
Wang, B., Lehmann, J., Hanley, K., Hestrin, R., Enders, A., 2015a. Adsorption and desorption of ammonium by maple wood biochar as a function of oxidation and pH. Chemosphere 138, 120–126.
Wang, B., Lehmann, J., Hanley, K., Hestrin, R., Enders, A., 2016. Ammonium retention by oxidized biochars produced at different pyrolysis temperatures and residence times. RSC Adv. 6, 41907–41913.
Wang, Z., Guo, H., Shen, F., Yang, G., Zhang, Y., Zeng, Y., Wang, L., Xiao, H., Deng, S., 2015b. Biochar produced from oak sawdust by Lanthanum (La)-involved pyrolysis for adsorption of ammonium (NH_4^+), nitrate (NO_3^-), and phosphate (PO_4^{3-}). Chemosphere 119, 646–653.
Yao, Y., Gao, B., Chen, J., Yang, L., 2013a. Engineered biochar reclaiming phosphate from aqueous solutions: mechanisms and potential application as a slow-release fertilizer. Environ. Sci. Technol. 47, 8700–8708.
Yao, Y., Gao, B., Chen, J., Zhang, M., Inyang, M., Li, Y., Alva, A., Yang, L., 2013b. Engineered carbon (biochar) prepared by direct pyrolysis of Mg-accumulated tomato tissues: characterization and phosphate removal potential. Bioresour. Technol. 138, 8–13.
Yao, Y., Gao, B., Inyang, M., Zimmerman, A.R., Cao, X., Pullammanappallil, P., Yang, L., 2011a. Biochar derived from anaerobically digested sugar beet tailings: characterization and phosphate removal potential. Bioresour. Technol. 102, 6273–6278.
Yao, Y., Gao, B., Inyang, M., Zimmerman, A.R., Cao, X., Pullammanappallil, P., Yang, L., 2011b. Removal of phosphate from aqueous solution by biochar derived from anaerobically digested sugar beet tailings. J. Hazard Mater. 190, 501–507.
Yin, Q., Ren, H., Wang, R., Zhao, Z., 2018. Evaluation of nitrate and phosphate adsorption on Al-modified biochar: influence of Al content. Sci. Total Environ. 631–632, 895–903.
Zhang, J., Shen, Z., Shan, W., Mei, Z., Wang, W., 2011. Adsorption behavior of phosphate on lanthanum(III)-coordinated diamino-functionalized 3D hybrid mesoporous silicates material. J. Hazard Mater. 186, 76–83.
Zhang, M., Gao, B., 2013. Removal of arsenic, methylene blue, and phosphate by biochar/AlOOH nanocomposite. Chem. Eng. J. 226, 286–292.
Zhang, M., Gao, B., Yao, Y., Inyang, M., 2013. Phosphate removal ability of biochar/MgAl-LDH ultra-fine composites prepared by liquid-phase deposition. Chemosphere 92, 1042–1047.
Zhang, M., Gao, B., Yao, Y., Xue, Y., Inyang, M., 2012. Synthesis of porous MgO-biochar nanocomposites for removal of phosphate and nitrate from aqueous solutions. Chem. Eng. J. 210, 26–32.
Zhang, Y., Guo, X., Wu, F., Yao, Y., Yuan, Y., Bi, X., Luo, X., Shahbazian-Yassar, R., Zhang, C., Amine, K., 2016. Mesocarbon microbead carbon-supported magnesium hydroxide nanoparticles: turning spent Li-ion battery anode into a highly efficient phosphate adsorbent for wastewater treatment. ACS Appl.Mater.Inter. 8, 21315–21325.
Zheng, Y., Wang, B., Wester, A.E., Chen, J., He, F., Chen, H., Gao, B., 2019. Reclaiming phosphorus from secondary treated municipal wastewater with engineered biochar. Chem. Eng. J. 362, 460–468.